catalysts

MDPI

Article

TiO_2 and Active Coated Glass Photodegradation of Ibuprofen

Samer Khalaf [1,2,*], Jawad H. Shoqeir [1], Filomena Lelario [2], Sabino A. Bufo [2], Rafik Karaman [2,3] and Laura Scrano [4]

1 Soil & Hydrology Research Lab (SHR), Department of Earth and Environmental Sciences, Al-Quds University, 20002 Jerusalem, Palestine; jhassan@staff.alquds.edu
2 Department of Sciences, University of Basilicata, Viadell'AteneoLucano 10, 85100 Potenza, Italy; filomenalelario@hotmail.com (F.L.); sabino.bufo@unibas.it (S.A.B.); dr_karaman@yahoo.com (R.K.)
3 Department of Bioorganic Chemistry, Faculty of Pharmacy, Al-Quds University, 20002 Jerusalem, Palestine
4 Department of European Cultures (DICEM), University of Basilicata, Via dell'AteneoLucano10, 85100 Potenza, Italy; laura.scrano@unibas.it
* Correspondence: skhalaf@staff.alquds.edu; Tel.: +970-598-600-781

Received: 29 January 2020; Accepted: 25 February 2020; Published: 18 May 2020

Abstract: Commercial non-steroidal anti-inflammatory drugs (NSAIDs) are considered as toxic to the environment since they induce side effects when consumed by humans or aquatic life. Ibuprofen is a member of the NSAID family and is widely used as an anti-inflammatory and painkiller agent. Photolysis is a potentially important method of degradation for several emerging contaminants, and individual compounds can undergo photolysis to various degrees, depending on their chemical structure. The efficiency oftitanium dioxide (TiO_2) and photocatalysis was investigated for the removal of ibuprofen from the aquatic environment, and the performance of these different processes was evaluated. In heterogeneous photocatalysis, two experiments were carried out using TiO_2 as (i) dispersed powder, and (ii) TiO_2 immobilized on the active surface of commercial coated glass. The kinetics of each photoreaction was determined, and the identification of the photoproducts was carried out by liquid chromatography coupled with Fourier-transform ion cyclotron resonance mass spectrometry (LC-FTICR MS). The overall results suggest that the TiO_2 active thin layer immobilized on the glass substrate can avoid recovery problems related to the use of TiO_2 powder in heterogeneous photocatalysis and may be a promising tool toward protecting the environment from emerging contaminants such as ibuprofen and its derivatives.

Keywords: ibuprofen; advanced oxidation process; TiO_2; photocatalysis; active glass

1. Introduction

Emerging contaminants resulting from the presence and circulation of pharmaceuticals (PhCs) were the focus of many environmental chemists over the last few decades. In the aquatic environment, PhCs are introduced anthropogenically through pharmaceutical or conventional plants [1]. PhCsare found in tiny concentrations in surface waters, indicating insufficient treatment of such entities during the standard sewage treatment processes (STPs). The occurrence of these toxic drugsin wastewater effluent, along with their metabolites which may be much more harmful than their parent compounds [2,3], has the potential to be a great health problem since they are endocrine-disrupting agents, thus posing a significant barrier to the use of water recycling [4].

Ibuprofen (IBP), (*RS*)-2-(4-(2-methylpropyl) phenyl) propanoic acid, shown in Figure 1, is a non-steroidal anti-inflammatory drug(NSAID) belonging to the class of propanoic acid derivatives used as pain relief for several inflammation conditions, including rheumatoid arthritis, asan analgesic

for pain relief in general, and as an antipyretic to help in fever conditions [5]. IBP enters the aquatic environment through effluents exiting secondary wastewater treatment plants, which are inefficient in removing a variety of small organic molecules, particularly pharmaceuticals [6]. Reported studies showed that the concentrations of IBP found in rivers and other environmental waters range between 10 ng·L^{-1} and 169 µg·L^{-1} [7].

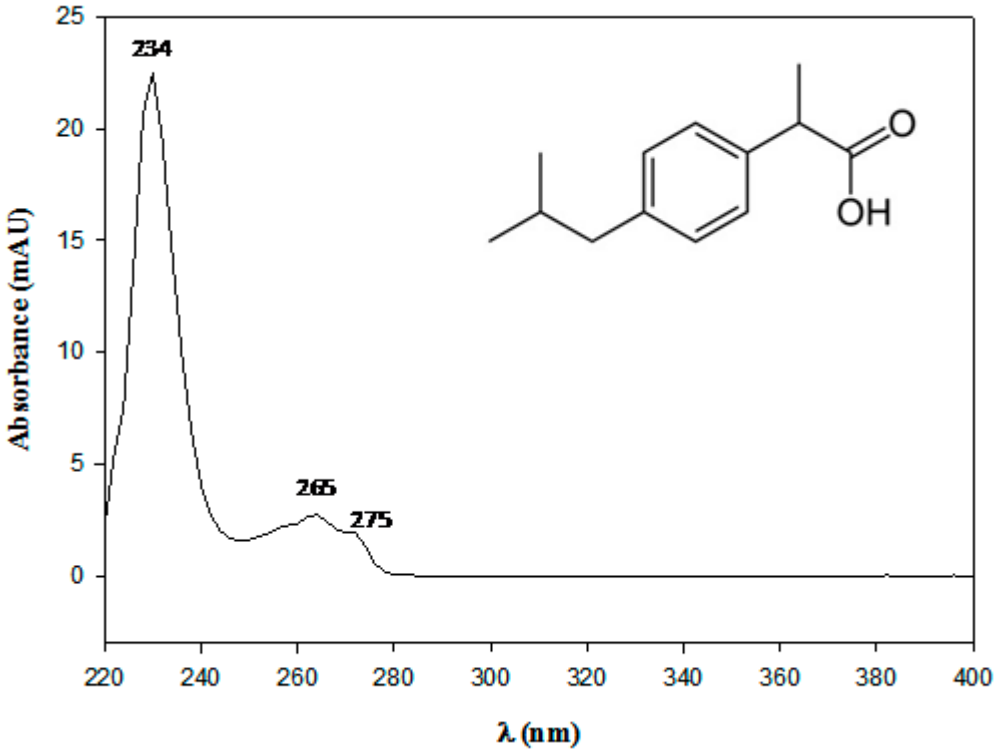

Figure 1. Chemical structure and ultraviolet (UV) absorbance of ibuprofen (IBP).

The fact that the current conventional wastewater treatment technologies such as those based on biological, thermal, and physical treatment processes are not efficient in removing or degrading small-molecular-weight pharmaceuticals with low biodegradability and high chemical stability such as ibuprofen [8] encouraged us to devote considerable effort toward developing a novel purification method that can efficiently remove this recalcitrant organic contaminant from the water environment.

Recently, we found that the integration of separation technologies, consisting of sequential elements of ultra-filtration (UF), activated carbon filtration (AC), and reverse osmosis (RO), as well as adsorption technology based on a surface modified clay minerals, was efficient in removing IBP and other pharmaceuticals to a safe level [9–13]. Nevertheless, the operating principles of these tools are only based on phase-transfer technologies, whereby the contaminant is retained on the filter or adsorbent without being degraded or destroyed to non-toxic compounds. Furthermore, some of the technologies used, such as UF and RO, are too expensive to be adopted in most real environmental situations. For the abovementioned reasons, we successfully attempted to find a good alternative method (degradation via photocatalysis) to these technologies for removing such pollutants from the aquatic environment.

The growing awareness of the risk arising from the occurrence of toxic organic contaminants in the aquatic environment promoted the development of technologies, such as photodegradation, and other advanced oxidation processes (AOPs), for efficient destruction of organic toxic compounds that exist in water and wastewater, including PhCs [14–16].

AOPs, i.e., processes based on highly reactive species such as hydroxyl radical (•OH), can oxidize and mineralize practically every organic entity [3], yielding CO_2 and inorganic ions, thus resulting

in total destruction of the target pollutant [3,8,16]. Advanced oxidation processes (AOPs) involve several homogeneous and heterogeneous processes such as photolysis, photocatalysis, ozonation, electrochemical oxidation, photo-Fenton, wet air oxidation, and sonolysis [8,15,16]. The most popular and effective type of AOP employed in water and wastewater treatment is heterogeneous photocatalysis with semiconductors [17–19].

Heterogeneous photocatalysis is a process via which a photoreaction is accelerated by the presence of a catalyst (usually semiconductor). In order for this to occur, the dispersed solid particles of the semiconductor in the treated solutionshould absorb significant portions of the UV light, and, under radiation, they may be photo-excited and produce oxidizing agents from water and oxygen [19]. Generally, TiO_2 is considered the most efficient semiconductor to be employed in photocatalysis because of several factors including its low cost, low toxicity, chemical stability, large band gap, and high photosensitivity [8,16–19].

Under ultraviolet irradiation, TiO_2 as a semiconductor causes the jump of an electron (e−) from the valence band (VB) to the conduction band (CB), resulting in the formation of a positive hole (h+) at the site of the electron. In the presence of aqueous suspended TiO_2, the hole and electron can produce radicals of hydroxyl and superoxide that are very potent in the oxidation of many kinds of organic entities found in water sources, thereby leading to total degradation of these toxic organic agents. [20,21]. Equations (1)–(3) depict the formation reactions of the superoxide and hydroxyl radicals upon catalysis with TiO_2

$$TiO_2 + hv \rightarrow e_{CB-} + h_{VB+}. \quad (1)$$

$$H_2O + h_{VB+} \rightarrow OH^{\bullet} + H_{aq+}. \quad (2)$$

$$O_{2(ads)} + e_{CB-} \rightarrow O_2^{\bullet}\text{-(ads)} + H_2O + OH^{\bullet}. \quad (3)$$

In some processes, a complete degradation of organic pollutants requires the presence of a radiation source, oxidizing agent, and a semiconductor. Oxidation and reduction processes are promoted by photo-generated charge carriers resulting from the excitation of TiO_2 via photons with higher energy. Currently, this kind of photocatalysis is utilized to purify water [8,16–19].

Although photocatalytic degradation using suspensions of TiO_2 particles was extensively employed to catalyze different contaminants, such as drugs, and although it achieved good results in recent years, this technique fails to be widely used because of the high cost and difficulty in isolating the semiconductor from the mixture after degradation [8,16–19]. To find a way around the need for catalyst recovery via filtration, a different approach, consisting of catalyst immobilization on a stationary support, should be assessed. For fulfilling this aim, TiO_2 immobilized on different materials instead of the traditional powder was advocated and tested for obtaining a promising clean treatment method with a low cost [22–24].

In this study, the efficiency of two different systems, direct photolysis and heterogeneous photocatalysis (TiO_2 powder and TiO_2 immobilized on active glass), was investigated using simulated solar irradiation for the removal of IBP and its major photoproducts from the aqueous phase. The comparative performance of the adopted process was analyzed under the same experimental conditions, and the kinetics for each photodegradation reaction was evaluated. Moreover, major photoproducts were detected and identified via liquid chromatography coupled with Fourier-transform ion cyclotron resonance mass spectrometry (LC-FTICR MS).

It should be emphasized that the study on the photodegradation of IBP using an immobilized TiO_2 system can be regarded as representative of a process for the degradation of a variety of pollutants which impose a risk to the environment.

2. Results and Discussion

2.1. Characterization of Active TiO_2-Coated Glass

Figure 2A,B depict the SEM image of the active glass and the TiO_2 coating comb geometry on the glass surface, respectively. The TiO_2 film thickness was 397.2 nm, as shown in Figure 2A.

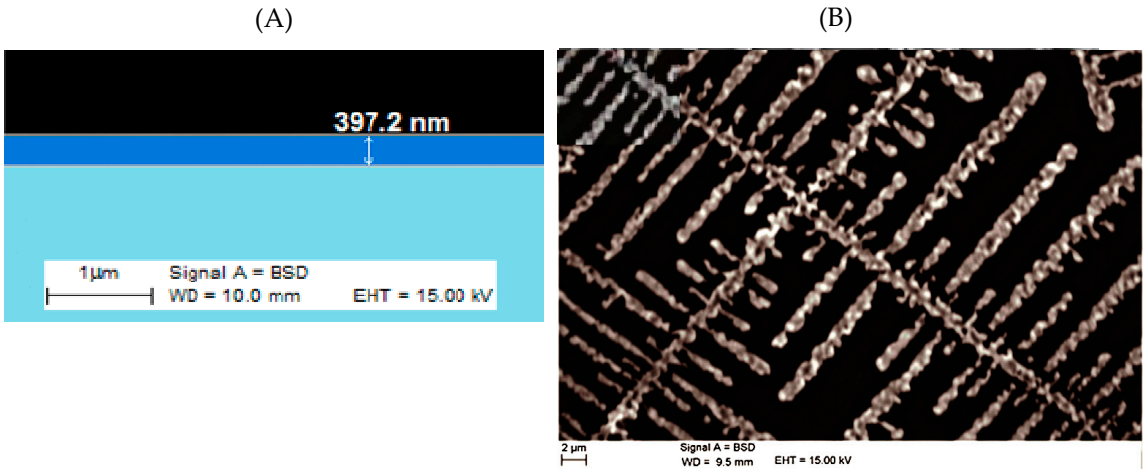

Figure 2. (**A**) SEM image of the blue glass cross-section illustrating the position of the TiO_2 layer immobilized on the glass surface; (**B**) SEM image of the blue glasssurface illustrating the fine-tooth comb nature of the TiO_2 coating.

Table 1 lists the elements in the glass surface and core class. As shown in the table, $TiO_2$is present only in the glass surface along with other elements, whereas it is absent in the core glass.

Table 1. Scanning electron microscopy EDX analysis of the glass surface coated with TiO_2 as compared to the glass core composition.

Elemental Composition of the Core Glass Energy: 6.686 KeV, Counts: 250		Elemental Composition of the Grafted Surface Energy: 6.686 KeV, Counts: 250	
Wt.% ± SD	**Elements**	**Wt.% ± SD**	**Elements**
47.2 ± 0.4	O	44.4 ± 0.4	O
36.2 ± 0.2	Si	38.6 ± 0.2	Si
4.3 ± 0.1	Na	6.0 ± 0.2	Na
6.0 ± 0.1	Ca	5.5 ± 0.2	Ca
2.4 ± 0.1	Mg	2.4 ± 0.1	Mg
2.1 ± 0.1	Sn	1.5 ± 0.1	Ti
0.3 ± 0.05	K	0.3 ± 0.05	K
1.0 ± 0.05	Al	0.3 ± 0.05	Al
0.4 ± 0.1	Fe	0.3 ± 0.05	Fe
0.1 ± 0.05	Cl	-	-

Sheel et al. (1998) reported the presence of cobalt oxide in a concentration of less than 75 µg/g [24], whereas we did not succeed in detecting any amount of cobalt oxide using our technique. It is believed that the blue color of the glass is due to the presence of cobalt oxide. For this reason, we report here the TiO_2-coated active glass using the abbreviation "blue glass".

The glass coating is based on photocatalytic anatase TiO_2, which is the most effective known photocatalyst [22,23]. For the preparation of the glass coating, TiO_2 nanocrystallinefilm is deposed onto float glass using an atmospheric pressure chemical vapor deposition technique (APCVD) as described in Reference [24]. Anatase is considered a more efficient photocatalyst than rutile because of its slower rate of recombination [23,24]. In the coated surface of the active glass, the catalyzing

efficiency is improved by the presence of Fe_3O_4, which favors the formation of multiple band gaps, enlarging the wavelength range that can be absorbed by the glass surface [22,23].

2.2. Photodegradation Experiments

2.2.1. Preliminary Study

Prior to photodegradation of IBP, which involves photolysis and photocatalysis experiments, thermal (45 °C) or hydrolytic reactions in pure IBP solution and the adsorption of the pharmaceutical on the catalyst surface in TiO_2 powder suspension were assessed. No significant loss of IBP occurred in dark conditions due to thermal reactions or hydrolysis. The adsorption equilibrium on TiO_2 powder was reached within 60 min, and a slight decrease (not more than 4.3%) of free IBP concentration in the 0.2–0.3 $g{\cdot}L^{-1}$ TiO_2 suspensions was achieved. Adsorption increased to 6.9% and more (7.8%) when the amount of TiO_2 powder was augmented to 0.4–0.5 $g{\cdot}L^{-1}$. The mentioned values are the average of three replicates.

2.2.2. Photolysis Experiment

The uranyl oxalate method [25,26] was used to assess the light emission effectiveness of the irradiation system prior to the experimental work. The disappearance of oxalate was 7.2×10^{-4} $mol{\cdot}s^{-1}$.

Despite the high efficiency of the irradiation system (irradiance to exposed surface of the reactor, 500 W/m^2), IBP concentration during this experiment was decreased only by 8.4% after more than 20 h. This result indicates that IBP is stable during photolysis because it has great chemical stability and a reduced molar adsorption coefficient above 280 nm [19] (Figure 1).

2.2.3. Photocatalysis Experiments

TiO_2 commercial powder and TiO_2-coated active glass were employed separately. The degradation efficiency via the two different methods was compared.

Photocatalytic Degradation Using TiO_2Powder

The concentration of IBP during the photocatalysis reaction was monitored using High Performance Liquid Chromatography-Ultra Violet HPLC-UV. The standard solution used showed a peak of IBP at 4.1 min retention time. After 5 min of sample irradiation, a marked decrease in the IBP concentration was observed (21.8% of the initial concentration) along with the appearance of a new photoproduct (Figure 3A,B).

After 30 min, a new peak due to the formation of another derivative was observed, and an approximately 60% reduction in IBP initial concentration was obtained (Figure 3C). Complete disappearance of IBP was achieved after 270 min (Figure 3D), while complete depletion including derivatives was observed after approximately 23hours (Figure 3E).

The combined results demonstrate that IBP was completely degraded by photocatalytic oxidation using TiO_2 powder under simulated solar irradiation, and the efficiency of its removal was more than 87% within 80 min. The degradation of IBP occurred as a result of a photo-irradiation of the semiconductor, causing an electron transfer to the conduction band which subsequently formed a hole in the valence band, which led to photo-induced charge separation on the semiconductor surface and an exchange of electrons on the water semiconductor interface. This led to the formation of $^{\bullet}O_2^-$ via interactions of adsorbed oxygen molecules with the photo-generated conduction band electrons, whereas the $^{\bullet}OH$ generated from the oxidation of the adsorbed water or hydroxyl anions by the valence band hole oxidized the adsorbed IBP molecules [17,19].

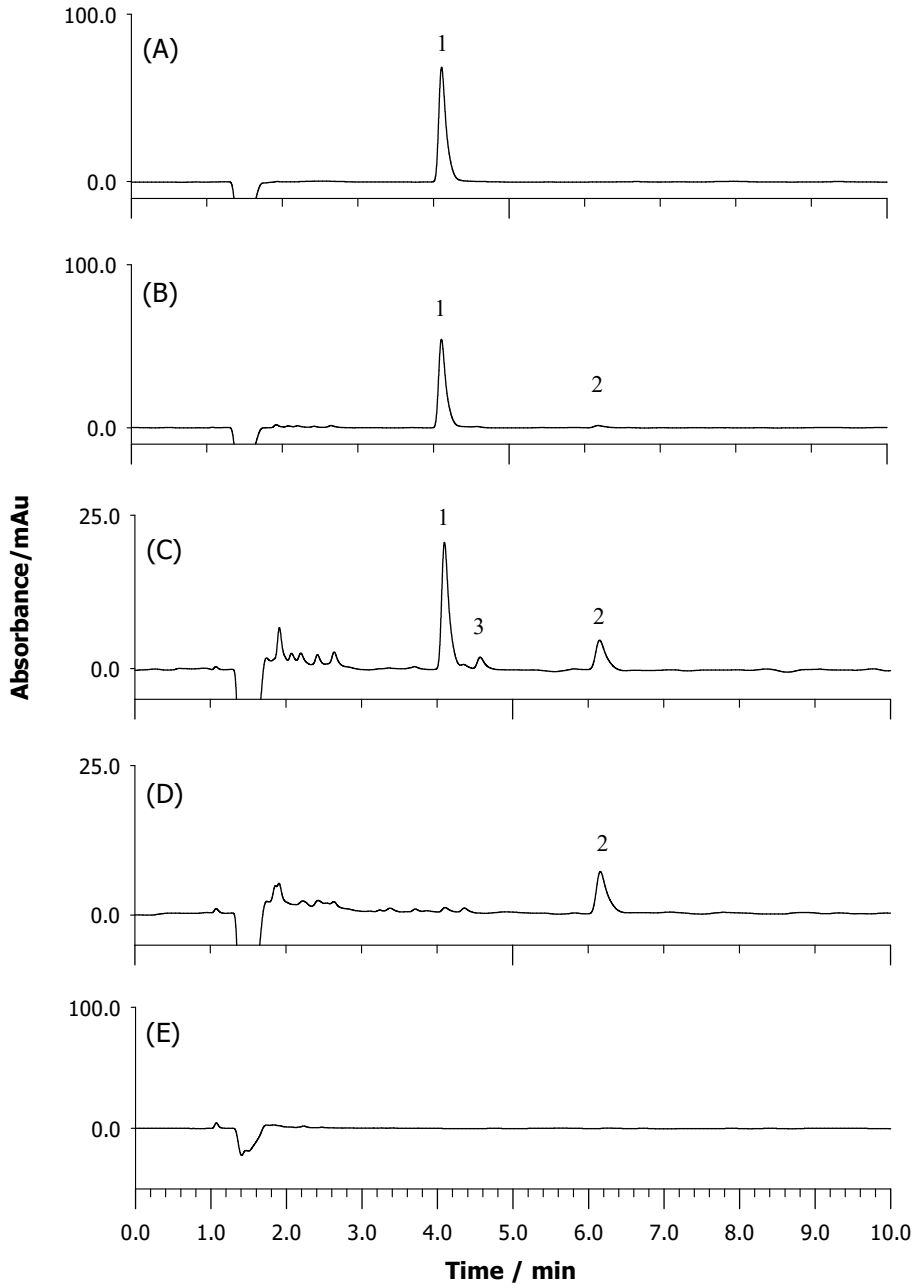

Figure 3. HPLC-UV separation of photodegraded solution using TiO_2 powder, IBP (1), and IBP photoproducts (2 and 3) (**A**) at time zero (initial standard solution), (**B**) after 5 min, (**C**) after 30 min, (**D**) after 270 min with complete disappearance of IBP, and (**E**) after 23 h with complete disappearance of IBP photoproducts.

Photocatalytic Degradation Using TiO_2-Coated Active Glass

During the first 2 h, a slight decrease in IBP concentration (2.7%) was achieved, while the appearance of a unique photoproduct was accomplished after 3 h (Figure 4A,B). Following a further 9hof irradiation, the concentration of IBP was decreased to 50%, and, after 24 h, IBP and its photoproduct disappeared (Figure 4C).

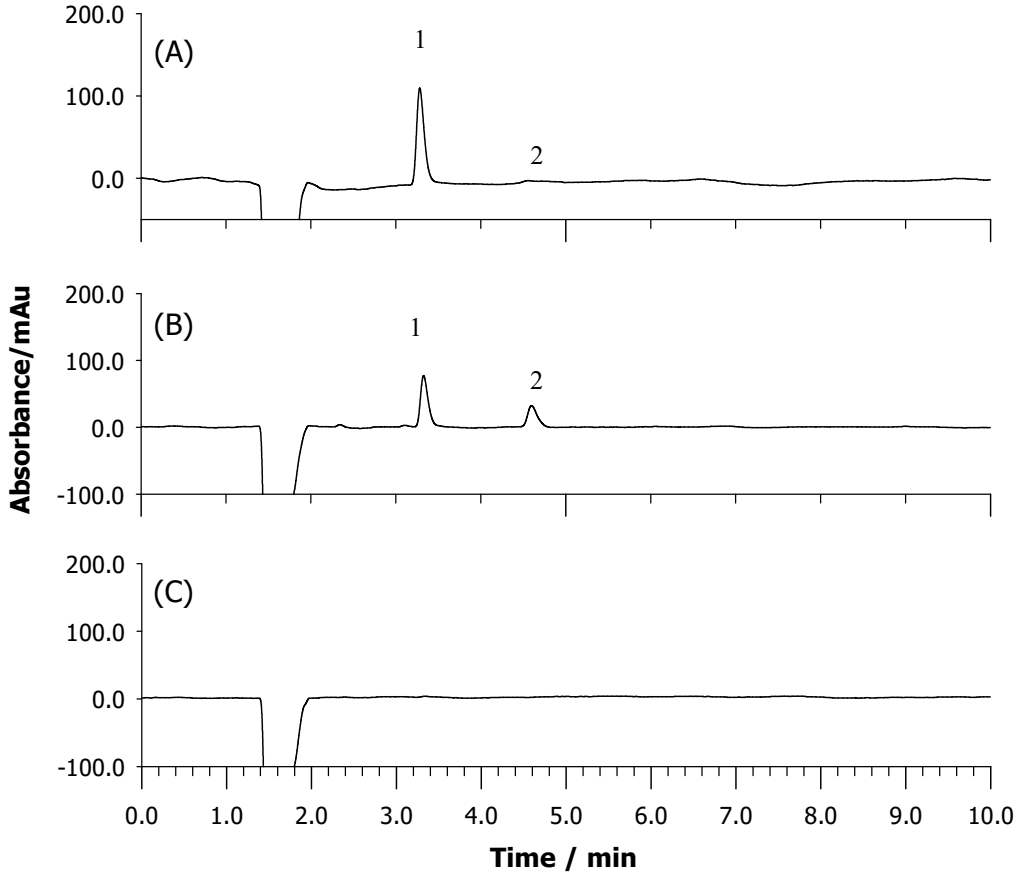

Figure 4. HPLC-UV separation of photo-degraded solution using TiO_2-coated blue glass, IBP (1), and IBP photoproducts (2) (**A**) after 180 min, (**B**) after 10 h, and (**C**) after 24 h with complete disappearance of IBP and IBP photoproducts.

2.3. Kinetics Studies

2.3.1. Experimental Observations

No degradation of IBP was observed in the dark in all aqueous environments adopted for the experiments. Direct photolysis under simulated sunlight did not achieve the desired goal. Accordingly, we can conclude that the direct interaction of IBP with sunlight (both via thermal hydrolytic reactions and photolysis) cannot lead to IBP's quick degradation. However, in the presence of TiO_2, complete removal of this NSAID was obtained although a xenon lamp with low UV energy was used for irradiation aiming at the simulation of sunlight effect.

Different amounts (0.1–0.5g·L^{-1}) of TiO_2 micro-particles were added to a solution of 25 mg·L^{-1} IBP to determine the efficiency of the catalytic process. The half-life (experimentally observed) of the mother molecule was reduced upon increasing the concentration of the catalyst from 0.1 to 0.2 g·L^{-1}, and it remained constant upon adding an amount of 0.3 g·L^{-1}, while it increased when concentrations of 0.4 or 0.5 g·L^{-1} were tested. The rationale behind such behavior is that the number of IBP molecules and photons absorbed on the TiO_2 particles increased with a moderate increase in the catalyst loading; however, with further addition of the semiconductor (powder), the phenomenon of light scattering took place and the number of useful photons per mass unit of TiO_2 was reduced. The disappearance of IBP at the highest concentrations of TiO_2 powder was mostly due to its mere physical adsorption onto the surface of semiconductor particles.

Figure 5A,B illustrates the depletion trend of IBP measured as C_t/C_0 versus irradiation time (A) and evolution of photoproducts (B) using different photodegradation methods. In both photocatalysis

processes, IBP underwent complete disappearance via the formation of one or two intermediates that were subsequently removed within 24 h.

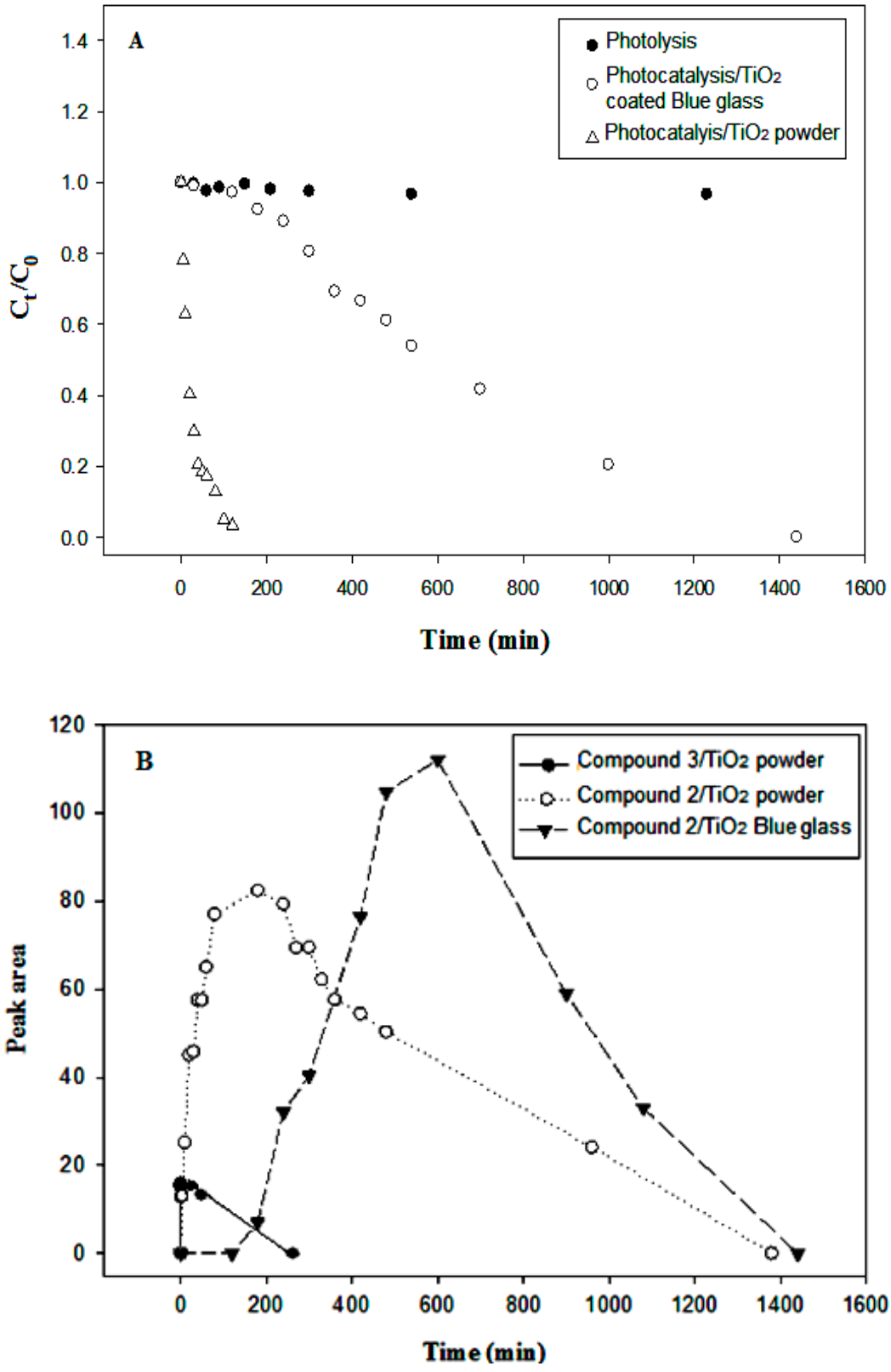

Figure 5. Evaluation of IBP degradation measured as C_t/C_0 versus irradiation time (**A**); evolution of photoproducts using different photodegradation methods (**B**).

In the photocatalysis experiment with TiO_2-coated active glass, the reaction was apparently slower than degradation obtained using TiO_2 powder, but a satisfactory depletion of IBP and its derivatives was reached in approximately the same time.

2.3.2. Kinetic Parameters

To find the kinetics model, kinetic parameters were calculated using integrated equations describing zero-, first-, and second-order (Langmuir-Hinshelwood) order equations [27]. According to Snedecor and Cochran (1989) [28], the least square method should be utilized to find the best fit.

Table 2 summarizes the kinetic parameters of IBP degradation under the photocatalysis experiment with TiO_2 powder.

Table 2. Kinetic parameters of IBP degradation under photocatalysis experiments.

Catalyzer	Reaction Order	Linearized Rate Equation	(ΣLSq)/n	k	$t_{1/2}$
TiO_2 powder	Zeroorder	$C_t = C_0 - kt$	12.47	0.2378 mg·L^{-1}·min^{-1}	37.6 min
	Firstorder	$\ln C_t = \ln C_0 - k\,t$	6.24	0.0251 min^{-1}	27.6 min
	Secondorder	$C_0/C_t = 1 + (1/t_{1/2})t$	0.18	0.0034 L·mg^{-1}·min^{-1}	11.8 min
TiO_2-coated active glass	Zeroorder	$C_t = C_0 - kt$	1.82	0.0124 mg·L^{-1}·min^{-1}	785 min
	Firstorder	$\ln C_t = \ln C_0 - kt$	0.05	0.0012 min^{-1}	575 min
	Secondorder	$C_0/C_t = 1 + (1/t_{1/2})t$	8.62	0.0001 L·mg^{-1}·min^{-1}	320 min

ΣLSq, sum of least squares = Σn (Cexp–Ccalc)^2; Cexp, experimental values of concentrations; Ccalc, value of concentrations calculated from rate equations; n, number of experimental observations; k, kinetic constant; $t_{1/2}$, half-life.

It must be taken into account that, owing to the dissimilar units associated with them, the values of kinetic constants calculated by equations describing reactions of different order cannot be compared. For this reason, it is useful to consider the values of half-life, which are always expressed in time units. Table 2 shows dissimilar values of the half-life when calculated using different equations applied to the same system. The least square method of estimation is a powerful method to assess the equation that can best fit the experimental data.

Apparently, the measured reaction rate of IBP under irradiation conditions using TiO_2 powder as a catalyst was best fit by a Langmuir–Hinshelwood-type equation [29].

$$Ct = C_0\, t_{1/2}/(t + t_{1/2}), \quad (4)$$

where C_0 is the initial amount (mg) of IBP per liter of solution, C_t is the remaining concentration at time t, and $t_{1/2}$ is the half-life of the reactant.

Equation (4) shows the minimum value of the sum of least squares, based on the number of observations (ΣLSq)/n, and describes a second-order reaction governed by the kinetic law.

$$\nu = -dC_t/dt = kC_t^2, \quad (5)$$

where ν is the reaction rate, and k is the rate (or kinetic) constant [27,29], which in our case can be calculated as

$$k = 1/(C_0 t_{1/2}). \quad (6)$$

Equation (5) represents a double dependence of the reaction velocity on the concentration.

The rationale behind such a finding may be due to the total reaction rate during the photocatalytic process being affected by two sorption states, both depending on the dissolved concentration of the pharmaceutical. The amount of reactant disappearing at each time t is affected by its free concentration in the powder suspension, as well as by the amount adsorbed on the catalyst particles, which depends on the remaining free concentration of IBP.

The half-life value for a second-order reaction, calculated by means of the linearized form of Equation (4) (Table 2), was just 11.8 min, while, after 80 min, 87% of IBP was converted.

The second-order kinetics shown in Figure 6A was confirmed by the linear behavior of (C_0/C_t) as a function of irradiation time (Figure 6B).

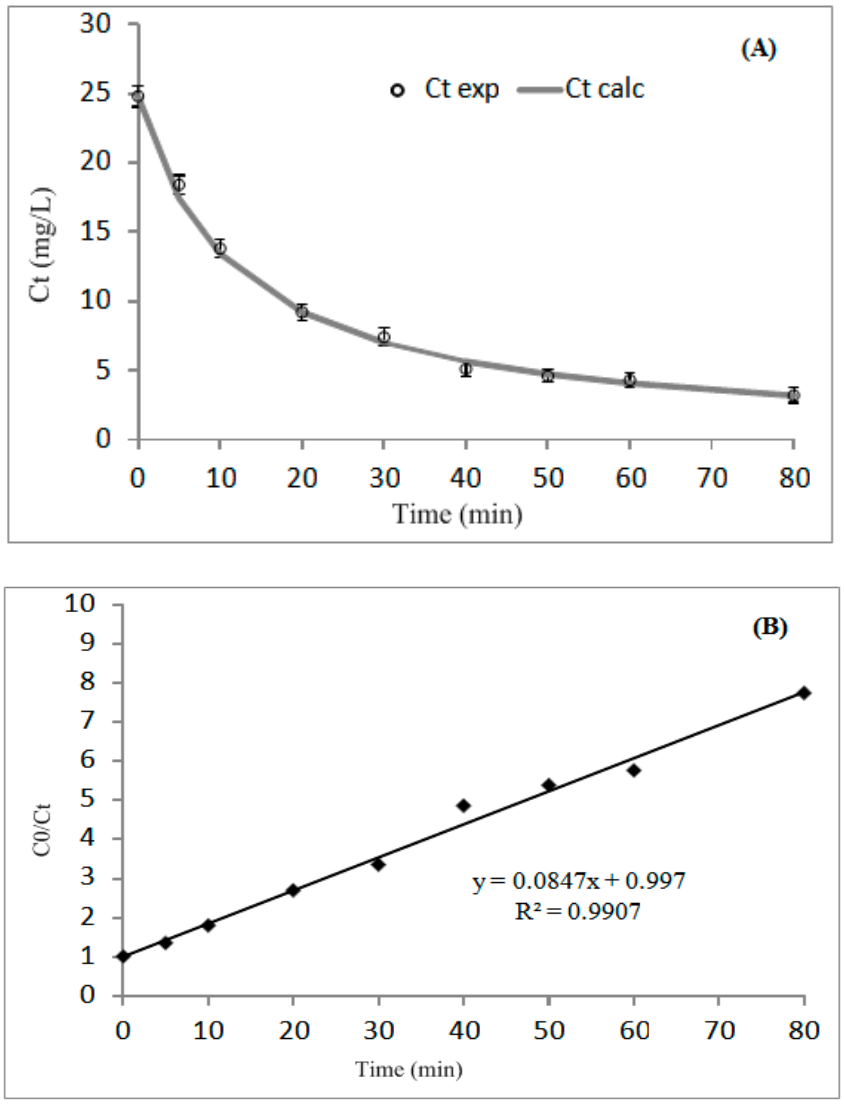

Figure 6. (**A**) Photodegradation of ibuprofen catalyzed by TiO_2 powder; Ct calc, values calculated using Equation (4); Ct exp, experimental values; error bars represent the standard deviations of three replicate experiments. (**B**) Trend of second-order linearized equation used for the calculation of kinetic parameters reported in Table 2.

From the results, it can be remarked that the initial degradation rate was high; however, it decreased rapidly as the reaction proceeded. The degradation was fast during the first 20 min, and then it gradually decreased; this trend is typical of second-order reactions. Several observations can be related to such a behavior: (1) the high concentration of IBP at the beginning of the reaction facilitates the useful attack by the hydroxyl radicals, resulting in high degradation rate; however, when IBP concentration gradually decreases, the degradation rate subsequently decelerates due to the dilution effect that reduces the possibility of useful collisions with the hydroxyl radicals; (2) the competitive reactions of the hydroxyl radicals with IBP degradation products that are produced during the reaction; (3) the recombination reactions of radical–radical.

The photodegradation reaction of IBP catalyzed by TiO_2 immobilized on active glass surface achieved 85% compound disappearance after 24 h of simulated solar light irradiation. By attempting to fit the concentration values vs. time using various-order integrated kinetic equations, it was found that the data best fit the first-order kinetic equation

$$C_t = C_0\, e^{-kt}. \quad (7)$$

In Figure 7A, the best fit of experimental data calculated using Equation (7) is represented clearly as confirmed by the high value of the determination coefficient (R^2) obtained for the linearized form of Equation (7) (Table 2, Figure 7B).

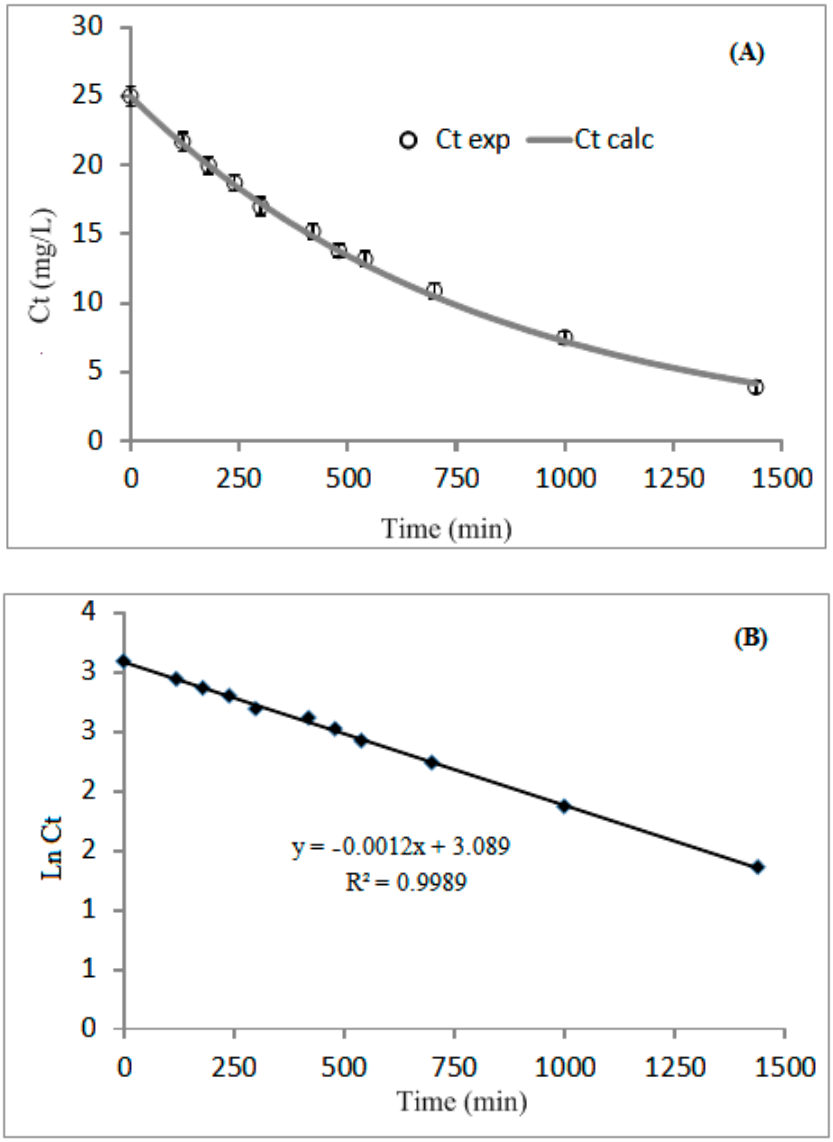

Figure 7. (**A**) Photodegradation of ibuprofen catalyzed by TiO_2-coated blue glass; $C_t$calc, values calculated using Equation (6); Ct exp, experimental values; error bars represent the standard deviations of three replicate experiments. (**B**) Trend of first-order linearized equation used for the calculation of kinetic parameters reported in Table 2.

In this case, the half-life can be calculated as

$$t_{1/2} = Ln2/k. \quad (8)$$

The value obtained was 575 min (Table 2), which is far from the half-life resulting from the experiment with TiO_2 powder; nevertheless, it is satisfactory if we consider the high stability shown by IBP molecules not only in the darkness (for testing thermal and hydrolysis degradation), but also under light irradiation (photolysis degradation). Moreover, from Equation (8), it is possible to notice that, unlike the case of the second-order reaction, the half-life for the first-order reaction does not depend on the initial concentration of the reactant. This means that the reaction catalyzed by TiO_2 immobilized on the active glass surface does not suffer from the same limitations encountered in the case of the second-order kinetics shown by IBP under the photoreaction catalyzed by TiO_2 powder dispersion (light scattering, radical–radical recombination reactions, and dilution effect). Furthermore, it should be emphasized that (i) the number and persistence of derivatives was reduced in the case of coated active glass, and (ii) the time needed for an efficient degradation of the mother drug and its derivatives was approximately the same.

We have to mention that the degradation of IBP is also influenced by the pH value of the medium [30]. The production of hydroxyl radicals is generally increased in an alkaline medium, since high concentrations of OH^- result in the formation of hydroxyl radicals, which are produced from the reaction of OH^- with TiO_2 on its surface's holes [31]. The pH value can also affect the charge on the catalyst particles; consequently, the electrostatic interactions between the charged surface of TiO_2 and the pollutant molecules can be largely influenced, thus leading to a change in the adsorption level of these molecules on the catalyst surface and interfacial electron transfer [32].The most dominant factor affecting the adsorption of pollutant on catalyst surface is the catalyst zero-point charge (zpc), which is defined as the pH at which the surface of the catalyst has neutral charge [33].

For TiO_2 P25 Evonik-Degussa, the zero-point charge value is 6.9. Therefore, the surface of TiO_2 is positively charged in acidic media and negatively charged in basic media [33]. Accordingly, the effect of pH depends mainly on the type of the pollutant and the zero = point charge of the semiconductor. As IBP is weakly acidic in nature, it is expected to be negatively charged at pH higher than 3 [30], while the TiO_2surface is positively charged at pH less than 6.9 [34]. Therefore, at pH = 4.5 where the photocatalytic experiment took place, the adsorption of IBP and, consequently, its photocatalytic oxidation were favored [30].

2.4. Identification of Intermediate Photoproducts

For the identification of IBP degradation byproducts, samples were collected at various time intervals and analyzed and identified by LC-FTICR MS system in the *m*/*z* range of 50–1000 in negative ionization mode. The results indicate the formation of two major photoproducts (Table 3). In addition, they reveal that the hydroxyl radicals attacked both the propionic acid and isobutyl substituent in IBP, resulting in the formation of two products, 2-[4-(1-hydroxyisobutyl) phenyl] propionic acid (2) and 4-(1-hydroxy isobutyl) acetophenone (3). Figure 8 depicts the proposed reaction pathways. The peak that appears at a nominal *m*/*z* value of 221, showing the formation of a mono-hydroxylated product of IBP, corresponds to 1-hydroxy IBP (2). Furthermore, product 2 was converted into another derivative with a nominal *m*/*z* value of 191, which corresponds to 4-(1-hydroxy isobutyl) acetophenone (3).

Table 3. Identification of ibuprofen and its photoproducts during photocatalytic degradation as deprotonated molecules, $[M–H]^-$, by high-resolution LC-ESI-FTICR MS.

No. [a]	Name	Accurate *m/z* [d] $[M–H]^-$	Molecular Formula [c] $[M–H]^-$	Rt [b] (min)	Error [e] (ppm)
1	ibuprofen	205.12343	$C_{13}H_{17}O_2^-$	4.1	0.14
2	1-hydroxy IBP	221.11835	$C_{13}H_{17}O_3^-$	6.2	0.13
3	4-(1-hydroxy isobutyl)acetophenone	191.10765	$C_{12}H_{15}O_2^-$	4.6	−0.50

[a] Number used to identify each compound in the chromatograms of Figures 4 and 5. [b] Chromatographic retention time of compounds eluted under the experimental conditions described in Section 3. [c] Molecular formula of deprotonated compound. [d] Accurate *m/z* value of deprotonated molecules. [e] Mass error in parts per million = $10^6 \times$ (accurate mass − exact mass)/exact mass.

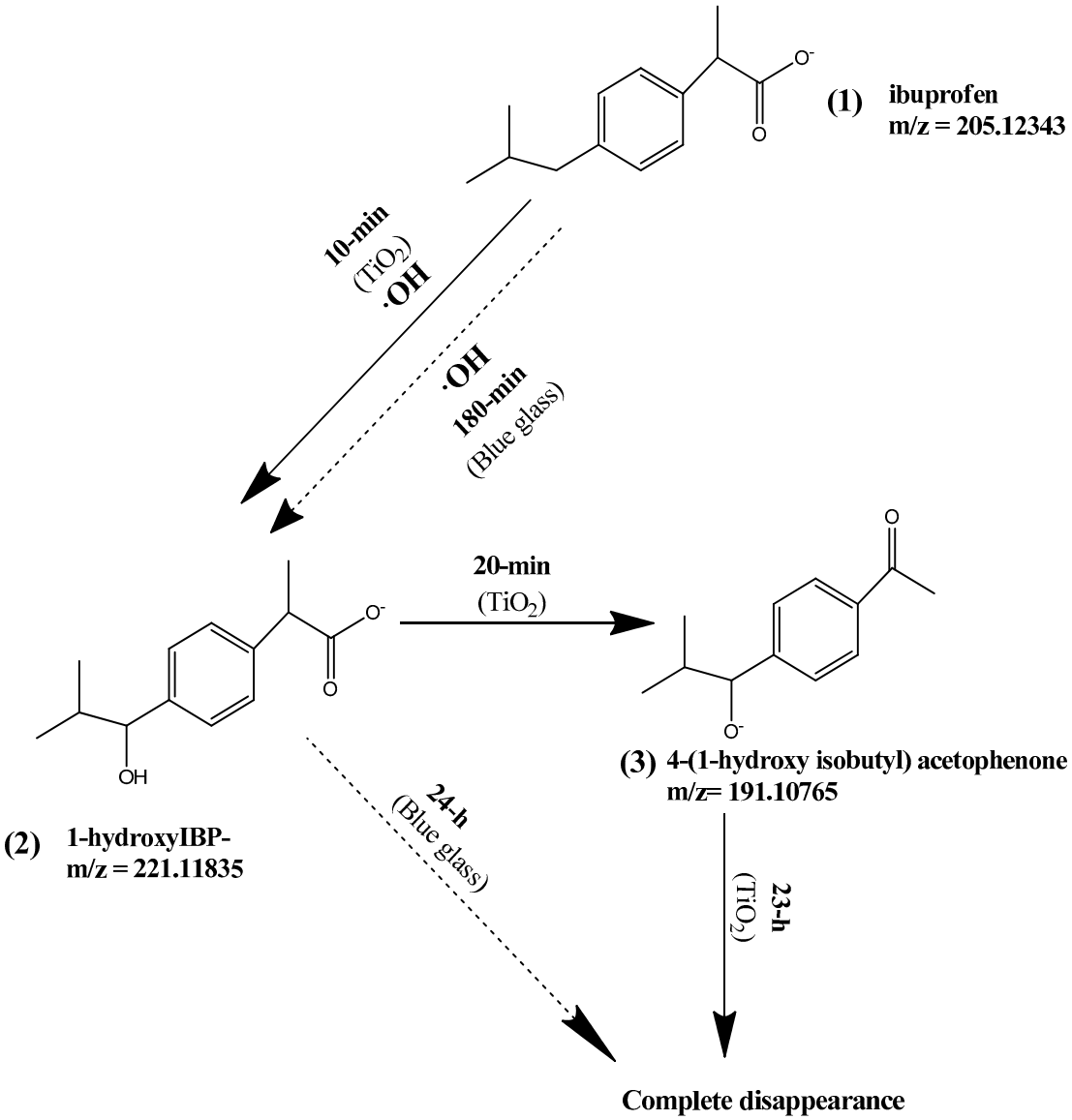

Figure 8. By-products generated by TiO_2 photocatalytic processes identified by LC-FTICR MS system in negative ion mode and proposed photodegradation pathway.

It is worth noting that, in the photodegradation method using TiO_2 immobilized on the active glass surface, only one by-product, compound 2, was detected.

3. Materials and Methods

3.1. Chemicals and Analytical Methods

Ibuprofen (MW, 206.3 g·mol^{-1}; pKa, 5.0) pure standard (purity, 99%) was purchased from Sigma Aldrich (Munich, Germany); acetonitrile, formic acid, and water for analysis were HPLC grade and purchased from Sigma Aldrich; TiO_2 Degussa P-25 was a kind compliment from Evonik Industries (Steinheim, Germany); TiO_2-coated active glass (Figure 9) was obtained as a gift from Pilkington (UK) (Sheel et al. 1998). PTFE (polytetrafluoroethylene) filters, 0.2 µm pore size, filter-Ø: 25mm, were purchased from Macherey-Nagel GmbH & Co. KG (Duren, Germany). Daily fresh working solutions were prepared using ultra-pure water from a bi-distilled purification system.

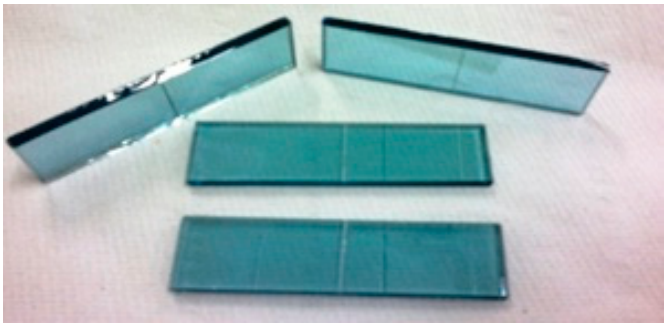

Figure 9. TiO_2-coated blue glass.

To avoid microbial contamination, all glass apparatus was heat-sterilized by autoclaving for 60 min at 121 °C before use. Aseptic handling materials and laboratory facilities were used throughout the study to maintain sterility.

IBP concentrations were monitored using high-performance liquid chromatography (HPLC) (1200 series, Agilent Technologies, Santa Clara, USA) equipped with an Eclipse XDB-C18 (3 µm particle size, 4.6 × 150 mm) column (Phenomenex, Torrance, USA) using a diode array detector (DAD) at a wavelength of 230 nm. The mobile phase consisted of 40% of 1% formic acid solution/60% acetonitrile. The flow rate was 1.0 mL·min^{-1}. Several aqueous solutions (from 0.5 to 25.0 mg·L^{-1}) of IBP were filtered, and 20 µL of the filtrate was injected and analyzed. Peak areas vs. concentration of IBP were plotted, and the calibration curve was obtained with a determination coefficient (R^2) of 0.9986. The limit of detection (LOD) of IBP for this method (using DAD) was 0.2 mg·L^{-1}, and the limit of quantitation (LOQ) was 0.6 mg·L^{-1}. The identification of IBP photoproducts was performed using the LC-FTICR MS system (Thermo Fisher Scientific, Bremen, Germany), in the same separation conditions. Negative ion ESI-MS mode was used for the detection of the compounds of interest. Full-scan experiments were performed in the ICR trapping cell in the range *m*/*z* 50–1000. Mass-to-charge ratio signals (*m*/*z*) were acquired as profile data at a resolution of 100,000 full width at half maximum (FWHM) at *m*/*z* 400. The limit of detection for mass spectrometric method was a few pmols.

The photodegradation experiments were performed using a solar simulator device Heraeus Sun-test CPS+ (Atlas, Chicago, USA), equipped with a 1500-W xenon arc lamp protected with a quartz filter (total passing wavelength: 280 nm < λ < 800 nm). The irradiation chamber was maintained at 20 °C by circulating water from a thermostatic bath and through a conditioned airflow.

3.2. Characterization of the TiO_2-Coated Active Glass

The active glass was obtained via a coating process using a nanocrystalline film of TiO_2 on a 4-mm-thin glass sheet. Some cross-sections obtained from theTiO_2-coated active glass were analyzed. The scanning electron analysis for the TiO_2-coated active glass was accomplished using a scanning electron microscope (SEM) of LEO model EVO50XVP, Carl Zeiss AG-EVO® 50 Series (Germany). The thin sections were grafted with 30-nm-thick carbon films. Semi-quantitative analyses of the

elemental composition of the different layers were obtained using a Ge ED Oxford-Link detector equipped with a super atmosphere thin window. Operating conditions of the SEM were as follows: 15 kV accelerating potential, 500 pA probe current, and about 10 mm working distance (WD). Thin sections of glass were prepared by the Department of Health and Environmental Science, Bari University. Samples were embedded in resin epoxy plugs and then polished.

3.3. Photolysis Experiment

Aqueous IBP solution of initial concentration 25 mg·L^{-1} was prepared by dissolving a determined quantity of standard IBP in ultrapure water. The measured pH of the solution was 4.5. The photolysis treatment was carried out in a glass Pyrex®batch reactor closed at the top with a quartz cover. IBP solution (250 mL) was placed into the reactor; then, thereactor was placed into the irradiation oven inside the solar simulator, which reproduced the spectral distribution of natural solar irradiation. The IBP solution was continuously remixed during the experiment by magnetic stirring, and samples were taken (1 mL for each sample) at determined intervals and then analyzed using the HPLC system according to the analysis method in Section 3.1. Three experiments of direct photolysis were performed in triplicate.

3.4. Photocatalysis Experiment with TiO_2Powder

A solution of ibuprofen was prepared as described in Section 3.3, but 50 mg of TiO_2 powder (0.2 g·L^{-1}) was added as the optimized amount in the reactor vessel. The aqueous suspension was mixed continuously in the dark for 2 h to ensure that the adsorption equilibrium of IBP on the catalyst surface was reached; then, the reactor was transferred into the solar simulator and exposed to solar irradiation, and samples were taken (1 mL for each sample) at determined intervals, then filtered and analyzed by HPLC. Three experiments were performed in triplicate.

3.5. Photocatalysis Experiment with TiO_2Immobilized on Active Glass

Seven active glass sheets were placed vertically to cover the full surface of the inner wall of the reactor; then, the solution of IBP, prepared as in the previous two experiments, was added, and the reactor was transferred into the solar simulator and exposed to xenon lamp irradiation with continuous mixing; samples were taken (1 mL for each sample) at determined intervals, and then filtered and analyzed. Three experiments were performed in triplicate.

4. Conclusions

IBP is very stable under direct photolysis conditions due to its high chemical stability and low molar adsorption coefficient in the range of wavelengths provided by solar irradiation. On the other hand, our experiments showed that effective destruction of IBP and its photoproducts is possible by photocatalysis in the presence of TiO_2 powder suspension or using TiO_2immobilizedon the surface of active glass. Two intermediate photo-products were detected and identified by LC-FTICR MS. As there is substantial equivalence in the long-term efficacy of photocatalys is in the presence of TiO_2 both as powder suspension and as glass coating, the use of active glass instead of TiO_2 suspension could be a promising technique for the removal of pharmaceutical residues such as IBP and its photoproducts from aquatic environments not requiring the recovery of the catalyst after photodegradation. To increase the effectiveness of the technique described herein, a modification of TiO_2immobilization on the glass surface using supports with a more complex geometry is essential.

Author Contributions: S.K. This work is a part of his PhD thesis (Chapter 4). Therefore all experiments and results and manuscript writing were referring to his own efforts; J.H.S. Supervision and reviewing results, reviewing the manuscript English writing; F.L. LCMS analysis; L.S. SEM analysis; S.A.B. Supervision and reviewing results, reviewing the manuscript English writing; R.K. Reviewing the manuscript English writing. All authors have read and agreed to the published version of the manuscript.

Funding: This work was supported by the European Union in the framework of the Project "Diffusion of nanotechnology-based devices for water treatment and recycling; NANOWAT" (ENPI CBC MED I-B/2.1/049, Grant No. 7/1997).

Acknowledgments: Many thanks to Jawad H. Shoqueir, the head of Soil and hydrology Lab at Al-Quds University, for his support to partially cover the publication fee from his own budget. Results reported in this article were partially presented by Samer Khalaf at the Second International Conference on Recycle and Reuse, 4–6 June 2014, Istanbul, Turkey and published in the book of abstracts.

Conflicts of Interest: The authors declare no conflict of interest.

References

1. Jorgensen, S.E.; Halling-Sorensen, B. Drugs in the environment. *Chemosphere* **2000**, *40*, 691–699. [CrossRef]
2. Oron, G.; Gillerman, L.; Bick, A.; Buriaskovsky, N.; Gargir, M.; Dolan, Y.; Mnoar, L.; Katz, L.; Hagin, J. Membrane technology for advanced wastewater reclamation for sustainable agriculture production. *Desalination* **2008**, *218*, 170–180. [CrossRef]
3. Renge, V.C.; Khedkar, S.V.; Thanvi, N.J. Photocatalytic-oxidation and reactors. *Int. J. Adv. Eng. Technol.* **2012**, *3*, 31–35.
4. Ahmed, S.; Rasul, M.G.; Martens, W.N.; Brown, R.; Hashib, M.A. Heterogeneous photocatalytic degradation of phenols in wastewater: A review on current status and developments. *Desalination* **2010**, *261*, 3–18. [CrossRef]
5. Madhavan, J.; Grieser, F.; Ashokkumar, M. Combined advanced oxidation processes for the synergistic degradation of ibuprofen in aqueous environments. *J. Hazard. Mater.* **2010**, *178*, 202–208. [CrossRef] [PubMed]
6. Richardson, M.L.; Bowron, J.M. The fate of pharmaceutical chemicals in the aquatic environment. *J. Pharm. Pharmacol.* **1985**, *37*, 1–12. [CrossRef] [PubMed]
7. Santos, J.L.; Aparicio, I.; Alonso, E. Occurrence and risk assessment of pharmaceutically active compounds in wastewater treatment plants: A case study: Seville city (Spain). *Environ. Int.* **2007**, *33*, 596–601. [CrossRef]
8. Klavarioti, M.; Mantzavinos, D.; Kassinos, D. Removal of residual pharmaceuticals from aqueous systems by advanced oxidation processes. *Environ. Int.* **2009**, *35*, 402–417. [CrossRef]
9. Karaman, R.; Khamis, M.; Qurie, M.; Halabieh, R.; Makharzeh, I.; Manassra, A.; Abbadi, J.; Qtait, A.; Bufo, S.A.; Nasser, A.; et al. Removal of diclofenac potassium from wastewater using clay-micelle complex. *J. Environ. Technol.* **2012**, *33*, 1279–1287. [CrossRef]
10. Khalaf, S.; Rimawi, F.; Khamis, M.; Zimmerman, D.; Shuali, U.; Nir, S.; Scrano, L.; Bufo, S.A.; Karaman, R. Efficiency of advanced wastewater treatment plant system and laboratory-scale micelle-clay filtration for the removal of ibuprofen residues. *J. Environ. Sci. Health Part B* **2013**, *48*, 814–821. [CrossRef]
11. Khalaf, S.; Rimawi, F.; Khamis, M.; Nir, S.; Bufo, S.A.; Scrano, L.; Mecca, G.; Karaman, R. Efficiency of membrane technology, activated charcoal, and a micelle-clay complex for removal of the acidic pharmaceutical mefenamic acid. *J. Environ. Sci. Health Part A* **2013**, *48*, 1655–1662. [CrossRef] [PubMed]
12. Qurie, M.; Khamis, M.; Malek, F.; Nir, S.; Bufo, S.A.; Scrano, L.; Karaman, R. Stability and removal of naproxen and its metabolite by advanced membrane wastewater treatment plant and micelle-clay complex. *Clean Soil Air Water* **2013**, *42*, 594–600. [CrossRef]
13. Sulaiman, S.; Khamis, M.; Nir, S.; Lelario, F.; Scrano, L.; Bufo, S.A.; Karaman, R. Stability and removal of dexamethasone sodium phosphate from wastewater using modified clays. *J. Environ. Technol.* **2014**, *35*, 1945–1955. [CrossRef] [PubMed]
14. Andreozzi, R.; Raffaele, M.; Nicklas, P. Pharmaceuticals in STP effluents and their solar photodegradation in aquatic environment. *Chemosphere* **2013**, *50*, 1319–1330. [CrossRef]
15. Inoue, M.; Masuda, Y.; Okada, F.; Sakurai, A.; Takahashi, I.; Sakakibara, M. Degradation of bisphenol A using sonochemical reactions. *Water Res.* **2008**, *42*, 1379–1386. [CrossRef]
16. Stathis, I.; Hela, D.G.; Scrano, L.; Lelario, F.; Emanuele, L.; Bufo, S.A. Novel imazethapyr detoxification applying advanced oxidation processes. *J. Environ. Sci. Health Part B* **2011**, *46*, 449–453.
17. Okamoto, K.I.; Yamamoto, Y.; Tanaka, H.; Tanaka, M. Heterogeneous decomposition of phenol over TiO_2 powder. *Bull. Chem. Soc. Jpn.* **1985**, *58*, 2015–2022. [CrossRef]
18. Phanikrishna Sharma, M.V.; DurgaKumari, V.; Subrahmanyam, M. TiO_2 supported over SBA-15: An efficient photocatalyst for the pesticide degradation using solar light. *Chemosphere* **2008**, *73*, 1562–1569. [CrossRef]

19. Zhu, X.; Yuan, C.; Bao, Y.; Yang, Y.; Wu, Y. Photocatalytic degradation of pesticide pyridaben on TiO_2 particles. *Int. Nano Lett.* **2005**, *229*, 95–105. [CrossRef]
20. Serpone, N.; Pellizetti, E. *Photocatalysis: Fundamentals &Applications*; John Wiley & Sons, Inc.: New York, NY, USA, 1989; pp. 604–634.
21. Stylidi, M.; Kondarides, D.I.; Verykios, X.E. Pathways of solar light-induced photocatalytic degradation of azo dyes in aqueous TiO_2 suspensions. *Appl. Catal. B Environ.* **2003**, *40*, 271–286. [CrossRef]
22. Mills, A.; Lepre, A.; Elliott, N.; Bhopal, S.; Parkin, I.P.; O'Neill, S.A. Characterisation of the photocatalyst Pilkington Activ(TM): A reference film photocatalyst? *J. Photochem. Photobiol. A* **2003**, *160*, 213–224. [CrossRef]
23. Parkin, I.P.; Palgrave, R.G. Self-cleaning coatings. *J. Mater. Chem.* **2005**, *15*, 1689–1698. [CrossRef]
24. Sheel, D.W.; McCurdy, R.J.; Hurst, S.J. Method of Depositing Tinoxideand Titanium Oxide Coatings on Flat Glass and the Resultingcoated Glass. Patent Application WO 98/06675, 19 February 1998.
25. Murov, S.L.; Carmichael, I.; Hug, G.L. *Handbook of Photochemistry*; Marcel Dekker: New York, NY, USA, 1993; pp. 82–99.
26. Volman, D.H.; Seed, J.R. The photochemistry of uranyl oxalate. *J. Am. Chem. Soc.* **1964**, *86*, 5095–5098. [CrossRef]
27. Scrano, L.; Bufo, S.A.; Perucci, P.; Meallier, P.; Mansour, M. Photolysis and hydrolysis of rimsulfuron. *Pestic. Sci.* **1999**, *55*, 955–961. [CrossRef]
28. Snedecor, G.W.; Cochran, W.G. *Statistical Methods*, 8th ed.; Iowa State University Press: Ames, IA, USA, 1989.
29. Scrano, L.; Bufo, S.A.; Emmelin, C.; Meallier, P. Abiotic Degradation of the Herbicide Rimsulfuron on Minerals and Soil. In *Environmental Chemistry: Green Chemistry and Pollutants in Ecosystems*; Lichtfouse, E., Schwarzbauer, J., Robert, D., Eds.; Springer: Berlin/Heidelberg, Germany, 2005; pp. 505–515.
30. Braz, F.S.; Silva, M.R.A.; Silva, F.S.; Andrade, S.J.; Fonseca, A.L.; Kondo, M.M. Photocatalytic Degradation of ibuprofen using TiO_2 and ecotoxicological assessment of degradation intermediates against daphnia similis. *J. Environ. Protect.* **2014**, *5*, 620–626. [CrossRef]
31. Chu, W.; Choy, W.K.; So, T.Y. The effect of solution pH and peroxide in the TiO2-induced photocatalysis of chlorinated aniline. *J. Hazard. Mater.* **2007**, *141*, 86–91. [CrossRef]
32. Chong, M.N.; Jin, B.; Chow, C.W.K.; Saint, C. Recent Developments in Photocatalytic Water Treatment Technology: A Review. *Water Resour.* **2010**, *44*, 2997–3027. [CrossRef]
33. Kosmulski, M. The significance of the difference in the point of zero charge between rutile and anatase. *Adv. Colloid Interface Sci.* **2002**, *99*, 255–264. [CrossRef]
34. Ning, B.; Graham, N.; Zhang, Y.P.; Nakonechny, M.; El-Din, M.G. The degradation of endocrine disrupting chemicals by ozone and AOPs—A review. *J. Ozone Sci. Eng.* **2007**, *29*, 153–176. [CrossRef]